STUDY OF THE INFLUENCE OF THE PROTECTION ARRANGEMENT ON PIEZO-ELECTRIC TRANSDUCERS APPLIED IN THE ELECTROMECHANICAL IMPEDANCE TECHNIQUE IN CONCRETE STRUCTURES

Lucas Gomes, Raquel Naira Fernandes Silva, Leila Aparecida de Castro Motta
Department of Civil Engineering, Universidade Federal de Uberlandia, Uberlandia, MG, 38.400-902, Brazil
lucas.g@ufu.br, raquelfernandes@ufu.br, lacastro@ufu.br

ABSTRACT

This paper presents an analysis of structural integrity monitoring using the electromechanical impedance method together with a finite element model. The objective is to implement and evaluate a protection arrangement for piezoelectric transducers, verifying their influence on damage detection. The methodology uses piezoelectric transducers embedded in the structure to acquire impedance signatures, where changes in the curve indicate potential damage. To identify the presence of damage, specific metrics are evaluated that allow detecting the presence of damage characterized by displacements in the signatures. The experiment compares a simulated model with a concrete sample tested in a controlled environment. The results show the correlation between the model values and those observed in the tests, evidencing the efficiency of the applied metrics.

KEYWORDS: *Structural health monitoring, Electromechanical impedance, Finite element method, Piezoelectric transducers.*

I. INTRODUCTION

Structural Health Monitoring (SHM) is based on the principle of characterizing damage to structures by means of a non-destructive testing method in the context of engineering, using it as a tool to assess the safety of structural components. The damage observed is characterized as the change in the dynamic properties of the structure, characterized as friction, fatigue, corrosion, cracks, among others, which significantly alter the behavior and performance of the elements. The typical implementation of the technique uses sensors that can be fixed to the surface or incorporated into the structural element to be monitored.

Different methodologies have been used for SHM, including acoustic emission, Lamb waves, fiber optic sensors, eddy currents and electromechanical impedance, among others observed in the literature [2]. The approach that allows the widest use is the use of piezoelectric patches of titanate and lead zirconate (PZT) coupled or incorporated into the structure of interest.

The signature of the PZT patch is measured taking into account a carefully selected frequency range, based on literature and experimental analyses that indicate high sensitivity to damage at frequencies between 50 and 80 kHz for metallic materials and from 10 to 400 kHz in heterogeneous materials such as concrete [11]. This selection also seeks to minimize the influence of environmental noise and ensure that the captured signatures are reliable for detecting structural variations. The real part of the signature suffers from the fact that it is more sensitive to temperature variations, and in addition to these points, other types of compensation must subsequently be implemented to mitigate distortions.

The fundamental principle of the SHM approach is to monitor changes in the structure's impedance signatures and correlate these changes with the existence of damage. To do this, damage metrics are used to quantify variations in impedance signatures. However, as mentioned, compensation techniques

based on damage metrics must be applied to the impedance signatures to compensate for the effects of temperature, with the aim of minimizing false positives (or false-negative alarms).

In this context, the present study focuses on the evaluation of the transducer protection assembly in conjunction with SHM and Finite element Method (FEM), using damage metrics to detect the presence of damage in a prism-type concrete structure. The results obtained are compared with consolidated damage using metrics such as root mean square deviation (RMSD) and correlation coefficient deviation (CCD) and mean absolute percentage deviation (MAPD), mitigating false positives (false negatives), distortions arising from environmental and operational changes.

The layout of this paper is organized as follows: Section II addresses the fundamentals of electromechanical impedance, damage characterization metrics, and the structure of the finite element method, as well as the properties of the materials. Section III presents the experimental program for validation of the simulation. Finally, Section IV summarizes the most important results of the study with suggestions for future research directions for improvement.

II. ELECTROMECHANICAL IMPEDANCE FOR STRUCTURAL MONITORING

2.1. Fundamentals of electromechanical impedance

SHM, together with the use of PZT transducers, aims to detect changes in structural properties, this change being characterized by the variation in the structure's electromechanical impedance. The transducer used is excited at a predefined frequency, generating a small deformation in the monitored structure which is transferred to the patch, which responds with a corresponding electrical response. The electrical variations correspond to the existence of damage in the structure.

The classical electromechanical impedance model consists of a system with one degree of freedom, in which the transducer can act as both actuator and receiver. The analytical model corresponding to Eq. (1) is expressed as the electrical admittance (inverse of the electrical impedance), Y (ω), of the transducer is directly correlated with the mechanical impedance of the structure, Zs(ω), and the transducer, Za (ω), and is evaluated in terms of the analysis range. In Figure 1 and demonstrating the one-dimensional analytical system in this context, we have that ZM (ω) represents the impedance, F (ω) is the alternating force, v (ω) is the resultant velocity and "ω" is the angular frequency. The mechanical impedance is expressed in Ohms (Ω).

$$Y(\omega) = \frac{I_0}{V_i} = G(\omega) + jB(\omega) = j\omega a\left[\varepsilon_{33}^{-T} - \frac{Z_s(\omega)}{Z_s(\omega) + Z_a(\omega)} d_{3x}^2 \hat{Y}_{xx}^E\right] \quad (1)$$

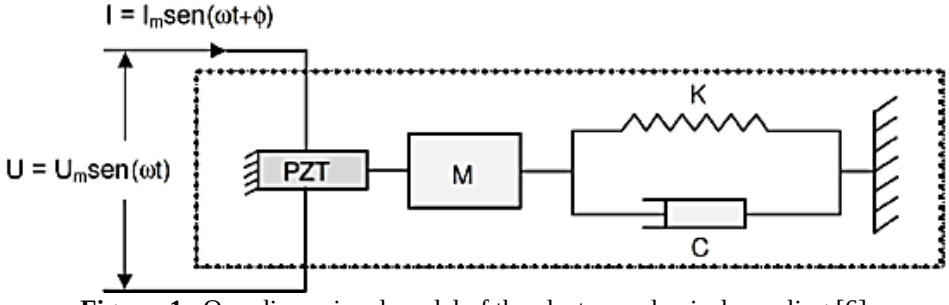

Figure 1. One-dimensional model of the electromechanical coupling [6].

For sensor purposes, we consider that C is the damping coefficient, K is the elastic constant of the spring and M is the mass. The transducer is excited by a sinusoidal voltage source U, where Um represents the amplitude and (ω) the angular frequency, producing a current I with amplitude and phase ϕ.The premise is that if the mechanical properties of the piezoelectric material (PZT) remain constant over time, fluctuations in its electrical impedance will be directly correlated with changes in the mechanical impedance of the monitored structure.

2.2. Damage metrics

The assessment and detection of damage uses the comparison of signatures, with the baseline being the representation of the structure in a healthy state, and subsequent collections as the actual state, in which they may (or may not) present variations characterized as damaged. The aforementioned signatures are compared using metrics (damage indices), comparing measurements taken at different times and establishing a scale based on statistical parameters. There are various damage detection techniques [10]. divided into modal indices and based on frequency response:

- Root Mean Square Deviation (RMSD)
- Mean Absolute Percentage Deviation (MAPD)
- Correlation Coefficient Deviation (CCD)
- Covariance (COV)
- Cube Correlation Coefficient Deviation (CCD3)
- Square or Euclidean norm (H2)

For this study, the RMSD, MAPD and CCD metrics are used to evaluate the behavior and measure the effectiveness of the signature's performance.

2.3. Finite element method

Modeling for transducer analysis consists of connecting analysis tools. Figure 2 illustrates the sequence for composing the model in COMSOL. For the numerical simulation, the piezoelectric sensor (PZT) was modeled as a hard disk with material properties representative of the PZT-4D, including density, Young's modulus, Poisson's ratio and dielectric damping. The transducer was coupled to the structure using a layer of epoxy resin.

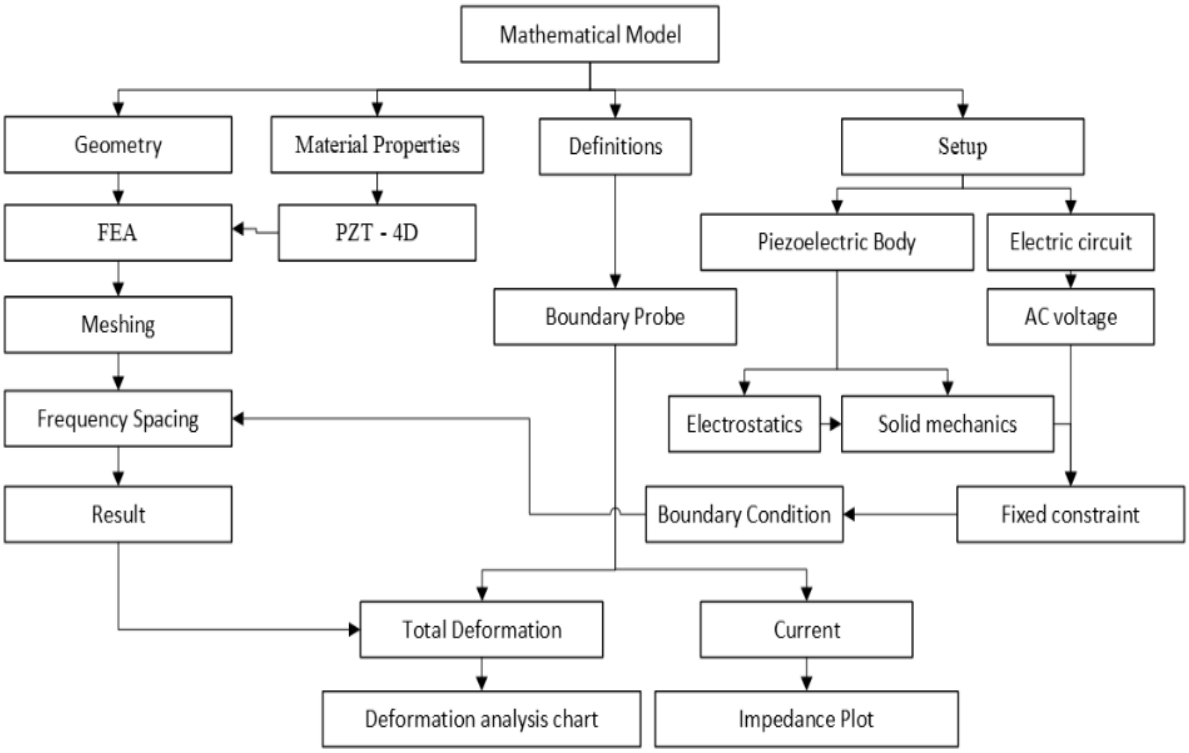

Figure 2. Dynamic finite element simulation process adapted [4].

For the numerical analysis, a free model was used to evaluate the response, using a PZT with a diameter of Ø25 mm and 0.7 mm, Figure 3 . The connection between the PZT and the structure was simulated using an intermediate layer of epoxy resin, with a uniform thickness of 0.2 mm, modeled to maximize

the transfer of mechanical energy and minimize distortions in the impedance data. A refined tetrahedral finite element mesh, with progressive refinement criteria around the transducer, was defined to capture stress and strain gradients with high precision. The model was validated against experimental configurations described in the literature using compatible material properties Table 1 and 2 [9].

Table 1: Properties of PZT-4D [3].

Parameters	**Symbols**	**Values**
Density	ρ	7600
Dielectric loss factor	$tan\delta$	0,0169
Compliance	$s_{11} = s_{22}$ s_{33} $s_{44} = s_{55}$ s_{66} s_{12} $s_{13} = s_{23}$	1,538 1,282 2,380 2,770 9,845 9,310
Relative electric permittivity	$\varepsilon_9 = \varepsilon_{22}$ ε_{33}	796,5 762,9
Piezoelectric stress coefficients	$d_{31} = d_{32}$ d_{33} d_{15}	-4,730 15.258 13,095

Properties used for the epoxy layer are illustrated in Table 2.

Table 2: Properties of epoxy resin. [5].

Parameters	**Variable**	**Value**
Young's modulus	E	2 GPa
Density	ρ	1250 kg/ m³
Poisson's ratio	v	0.40

The transducer parameters, according to the constitutive equations, are described using the nomenclature shown in Eq. (2) and Eq. (3) [1]:

$$S_2 = \bar{s}_{22}^{E}\, T_2 + \, d_{32}E \tag{2}$$

$$D_3 = \bar{\epsilon}_{33}^{T}\mathrm{E} + d_{32}T_2 \tag{3}$$

The parameters included are: S2 is the strain,D_3 is the electrical displacement,$\bar{s}_{22}^{E}$ is the complex compliance,T_2 is the stress;d_{32} is the piezoelectric constant, and$\bar{\epsilon}_{33}^{T}$ is the complex dielectric constant. This approach made it possible to observe how variations in the materials and the connection influence the system's response The analysis was carried out in the frequency domain to identify relevant resonance peaks.

Signatures were collected with a voltage set at 1V within the frequency range of 10kHz to 400kHz, a range observed in several studies [9,10]. This range is suitable for assessing the transducer's behavior accurately and comprehensively to detect one or more resonance peaks. A transducer with the same specifications used in the FEM was tested on a bench to check the settings and adjustment. The values obtained are exported by the equipment itself, with 801 points obtained using the Agilent 4294A impedance analyzer Figure 3 b shows the signature obtained by comparing the numerical model and the one obtained in an impedance analyzer test.

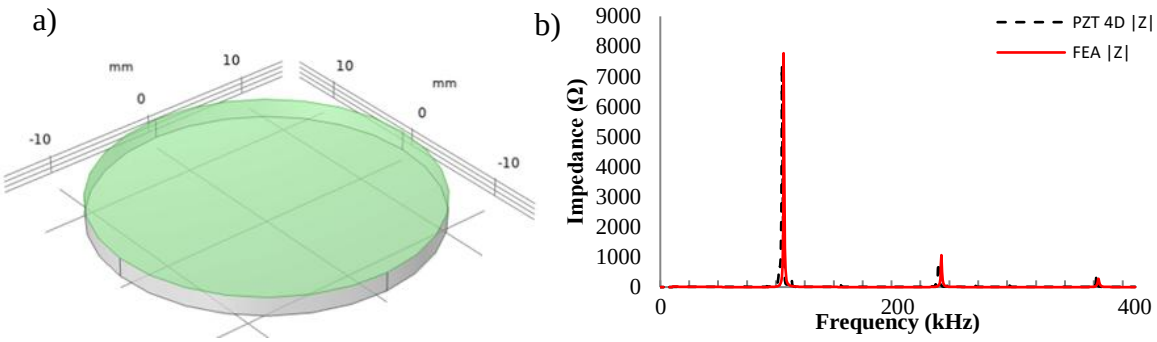

Figure 3. (a) Representation of the free 3D model (b) FEM and bench impedance.

Based on the initial analysis, the assembly is modeled incorporating the protective part, with the metal plate chosen as the initial study element. Together with the other materials, its properties are described in detail in Table 3.

Table 3: Properties of aluminum [3]

Parameters	Variable	Value
Young's modulus	E	70 GPa
Density	ρ	2700 kg/m³
Poisson's ratio	v	0.33

The structure proposed for creating the SIAU (Structural Integrity Analysis Unit) consists of a set of aluminum plates with a thickness of 0.6 mm and dimensions of 30x30 mm, epoxy and PZT-4D, as shown in Figure 4. The model is based on the assembly used in studies [8], which uses an epoxy coating to protect the transducer.

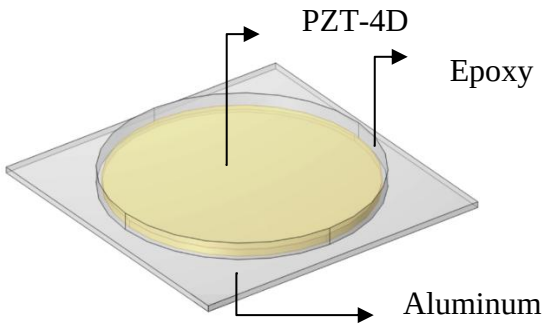

Figure 4. 3D model of the SIAU.

2.4. Numerical simulation of the influence of the protection arrangement

In this work, a prismatic specimen with a length of 500 mm, a width of 150 mm and a height of 150 mm was used. The experimental setup was evaluated using the FEM to analyze the behavior of the system under different damage conditions, keeping the PZT inside the structure for evaluation. Figure 5 shows the initial FEM model with the PZT embedded in epoxy resin, a standard commonly used in various protective research.

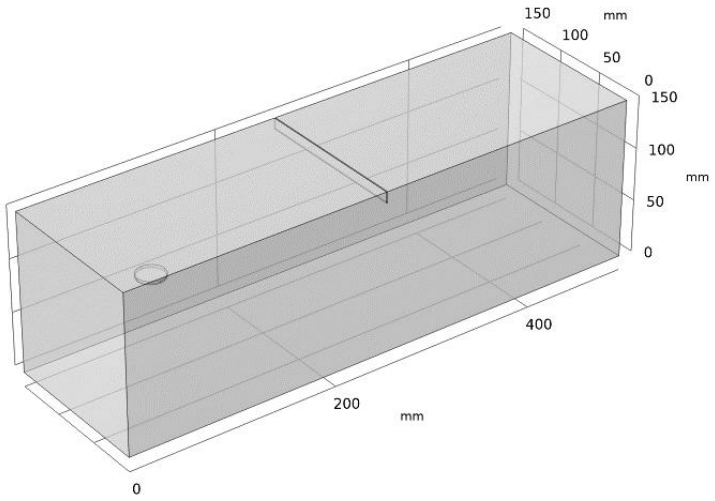

Figure 5. 3D model.

Subsequently, the model is visualized with the blade incorporated into the model to check the signatures, Figure 6. This approach made it possible to evaluate the impedance signatures obtained by the model.

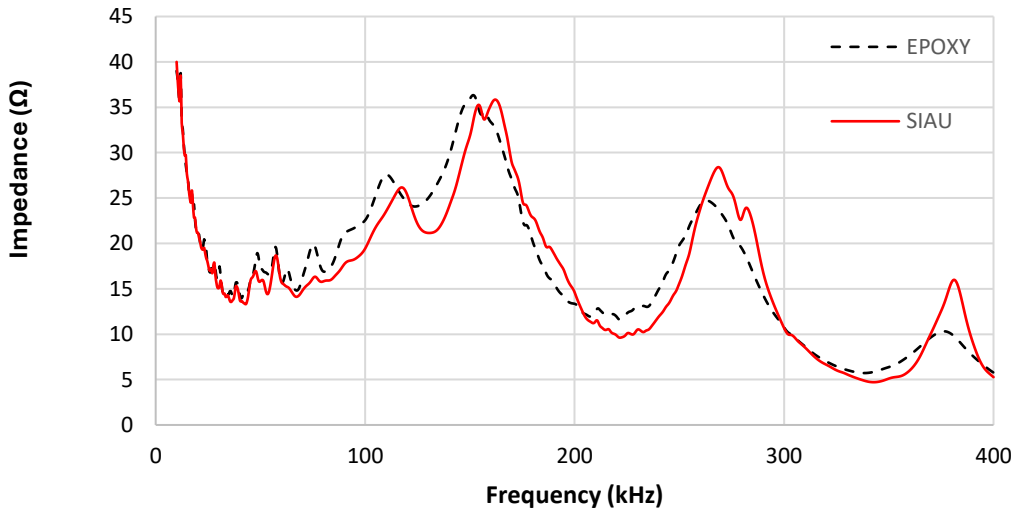

Figure 6. Impedance versus frequency signature of epoxy protection and SIAU.

The evaluation of the behavior can be verified by observing the impedance variation, which makes it clear that the addition of the element promotes an increase in the secondary and tertiary peaks observed in the 200-300kHz and 350-400kHz range compared to the epoxy protection. Using the same model as before, the influence of the epoxy and epoxy/aluminum foil protections on the detection of 10 mm damage in the central region was analyzed using MEF. The signatures obtained were compared with the baseline signatures, demonstrating the effectiveness of the different protections in detecting damage.

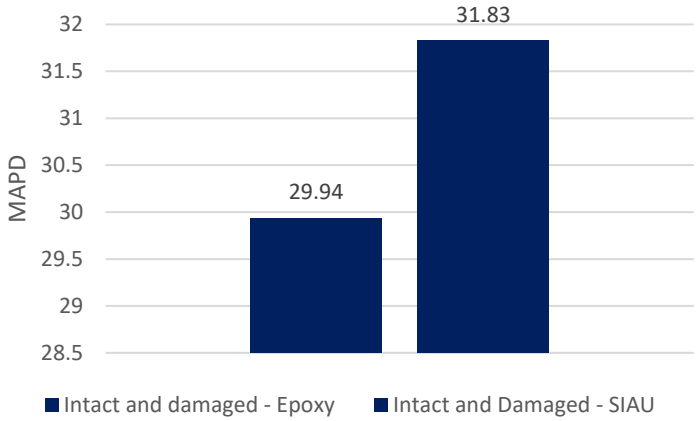

Figure 7. MAPD of the intact structure compared to damage with epoxy protection and SIAU.

As seen in Figure 7 the addition of the foil provides a significant improvement in the response in concrete structures when compared to simple epoxy protection.

III. EXPERIMENTAL VALIDATION

3.1 Structural test and measurement systems

For this evaluation, a 30 MPa prismatic concrete was molded in the laboratory using CP-V ARI, using the same dimensions as those used in the simulated model. The casting process included the use of standardized forms and the application of compaction techniques to minimize the presence of voids in the concrete, ensuring greater uniformity of the material.

After molding, the specimens were subjected to controlled curing for 28 days in a humid chamber and then placed for 2 days in an environment with a constant temperature of 25 °C (± 0.5 °C). This curing period is essential to allow the complete development of the concrete's mechanical properties before the functional tests are carried out. The layout of the (SIAU) followed the scheme seen in Figure 5, being positioned 125 mm from the side face. In this arrangement, the sensors were strategically positioned during the casting of the specimens to ensure adequate coverage of the area of interest and to allow precise monitoring of the structural responses over time.

Baseline signatures, as well as subsequent readings, were obtained using the Agilent 4294A impedance analyzer. During the data collection phase, 2403 data points were recorded, covering a wide frequency range, verifying the range (10 to 400kHz) further subdivided into three subintervals using 1V with 3 collection repetitions, applying sinusoidal excitation, in this analysis the equipment generated the excitation and the responses were calculated directly by the equipment. To validate repeatability, a new test was carried out with repetition over a 12-hour interval, confirming the stability of the measurements. This signature data was then analyzed to identify patterns and variations that could indicate the presence of damage, using the software to run the numerical routine using GNU Octave to determine the metrics (RMSD, MAPD and CCD).

3.2 Damage generation and testing

To assess the damage to the central section of the prismatic bodies, a GDC 151 wet marble saw was used to make precise cuts at depths of 10, 20 and 30 mm. Impedance signatures were collected at each depth using two different transducers: one with an aluminum blade attached and the other with a simple shield. This approach allowed a detailed comparison of the electromechanical impedance responses between the two types of transducers under different damage conditions. Figure 8 and Figure 9 show the layout of the section, the sensors and the 3D model, respectively.

Figure 8. Experimental prismatic sample with cut.

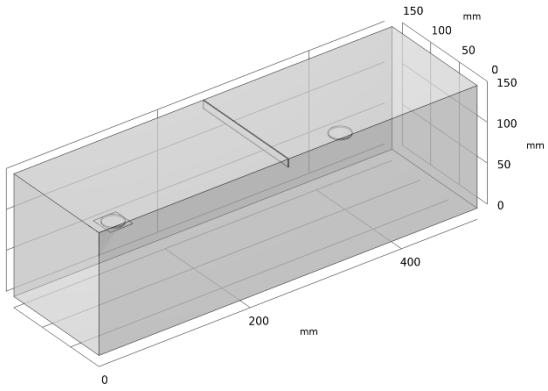

Figure 9. 3D model of damaged cut with SIAU and basic protection.

The signature obtained with the SIAU is illustrated in Figure 10 together with the presence of damage with the total frequency range from 10kHz to 400kHz, with two notable peaks. The first peak is commonly called the structure peak [7], these two points are used to analyze the behavior with the metrics. As illustrated in Figure 11, a cut of 40kHz to 200 kHz range of the signature, comparing the modeling results with the experimental results. The experimental validation demonstrated satisfactory correlation between the simulated models and the experimental results. However, it was possible to observe discrepancies in the secondary peaks, which can be attributed to the heterogeneity of the concrete, which is not completely captured in the numerical modeling. These differences reinforce the importance of adjusting the FEM model parameters, such as mesh density and boundary conditions, to better represent the real behavior of the structure.

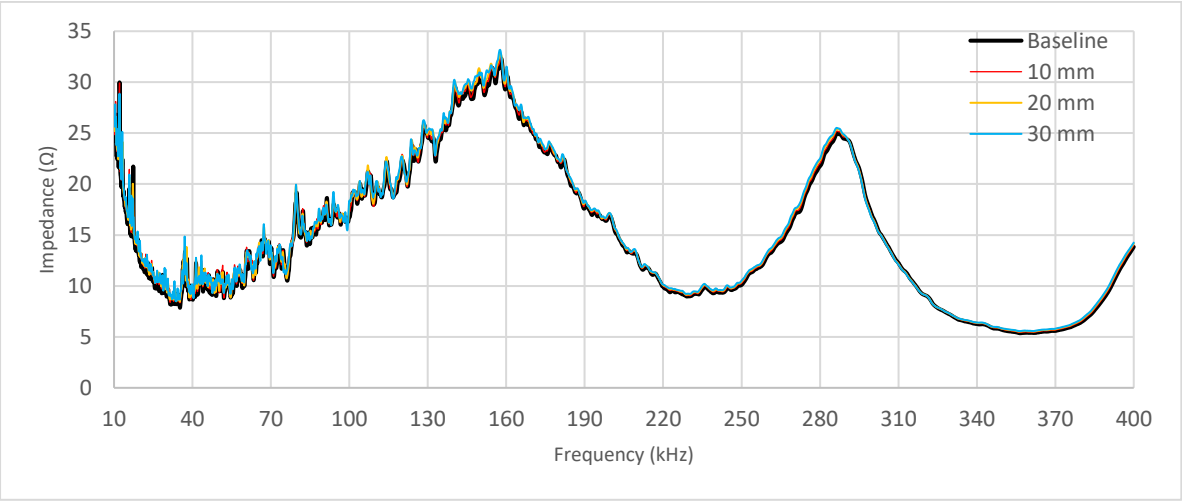

Figure 10. Impedance signature by SIAU frequency.

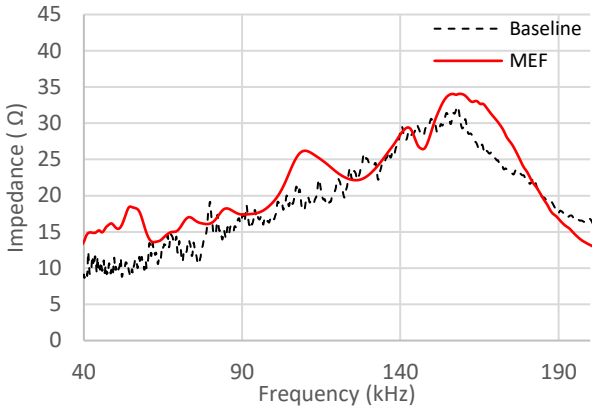

Figure 11. SIAU impedance signature and experiment.

The MAPD plot as a function of different notch depths in the sample, analyzing a full frequency range from 10 kHz to 400 kHz, is shown in Figure 12. This analysis includes experimental evaluation and simulation using FEM, with reference to undamaged elements. The data is compared between two different materials: SIAU and epoxy, with the aim of determining the effectiveness in detecting damage at different notch depths. The results demonstrate that increasing damage depth causes an increase in MAPD and CCD metrics in both protections evaluated. Comparing the materials, the SIAU set presented consistently higher MAPD values in all damage conditions, indicating greater sensitivity.

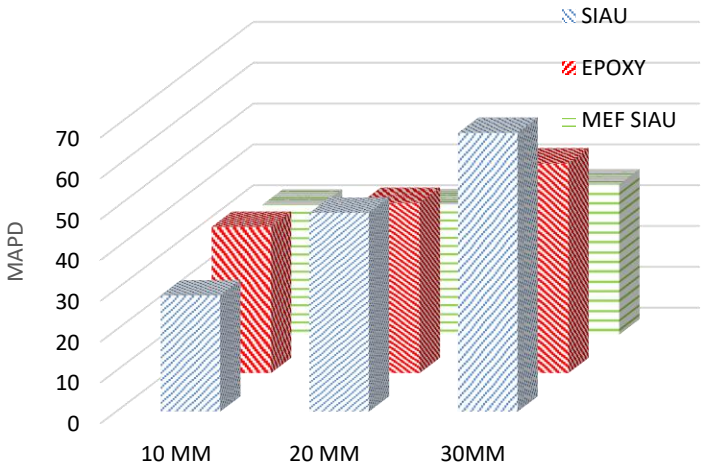

Figure 12. MAPD from 10kHz to 400kHz of the intact structure compared to damage with epoxy protection and SIAU.

FEM, on the other hand, has the lowest MAPD values, suggesting lower sensitivity. This variation in MAPD values between materials can be attributed to the different intrinsic characteristics of each material and the interaction with the technique used. The difference between the experimental results and the simulation may be due to the non-linear response of the specimen, which may not be completely captured by the modeling. The complete values of the metrics evaluated in the primary and secondary resonance peaks, ranging from 130kHz to 200kHz and from 260kHz to 320kHz, observed in the signatures of the experiments tested and taking the undamaged elements as a reference, are shown in Table 4.

Table 4 - RMSD, MAPD and CCD calculated for PZT.

Cutting Stage		Epoxy			SIAU		
		RMSD	MAPD	CCD	RMSD	MAPD	CCD
Resonance of peak 1	10 mm	2.896	9.085	0.741	0.207	2.271	0.332
	20 mm	2.898	9.070	0.741	0.445	4.982	0.423
	30 mm	3.753	11.750	0.962	0.620	7.032	0.546
Resonance of peak 2	10 mm	3.830	3.830	0.282	0.183	3.377	0.275
	20 mm	6.438	6.438	0.346	0.366	7.209	0.396
	30 mm	9.289	9.289	0.431	0.499	9.802	0.530

The analysis also demonstrated that the secondary resonance peak is more responsive to the presence of damage in SIAU configurations, while the primary peak is more reliable when using only epoxy. These differences reinforce the importance of selecting protective materials according to the characteristics of the monitored structure. The same behavior is observed with MAPD for damage detection. Regarding the RMSD values, it can be observed that the values are more expressive in the case of epoxy compared to the SIAU values.

Figure 13 shows the RMSD, MAPD and CCD values versus the evolution of the cutting steps and the R^2 coefficient used to verify the performance of the arrangement. For the first case, the positive correlation can be seen in Figure 13a, where the RMSD, MAPD and CCD values increase as the damage increases, all the values of the three metrics show a strong linear correlation, where the R^2 is greater than 0.99. In Figure 13b, the R^2 values are close to 0.75, with a positive trend, but not establishing a strong linear correlation compared to the SIAU in the first range. Figure 13c, the second peak, shows the same correlation with the first range. In Figure 13d, it can be seen that the behavior has become more linear compared to the first range, where the R^2 is greater than 0.99. In general, it can be seen that the addition of the blade provides better performance in correcting the evolution of the damage in the metrics analyzed.

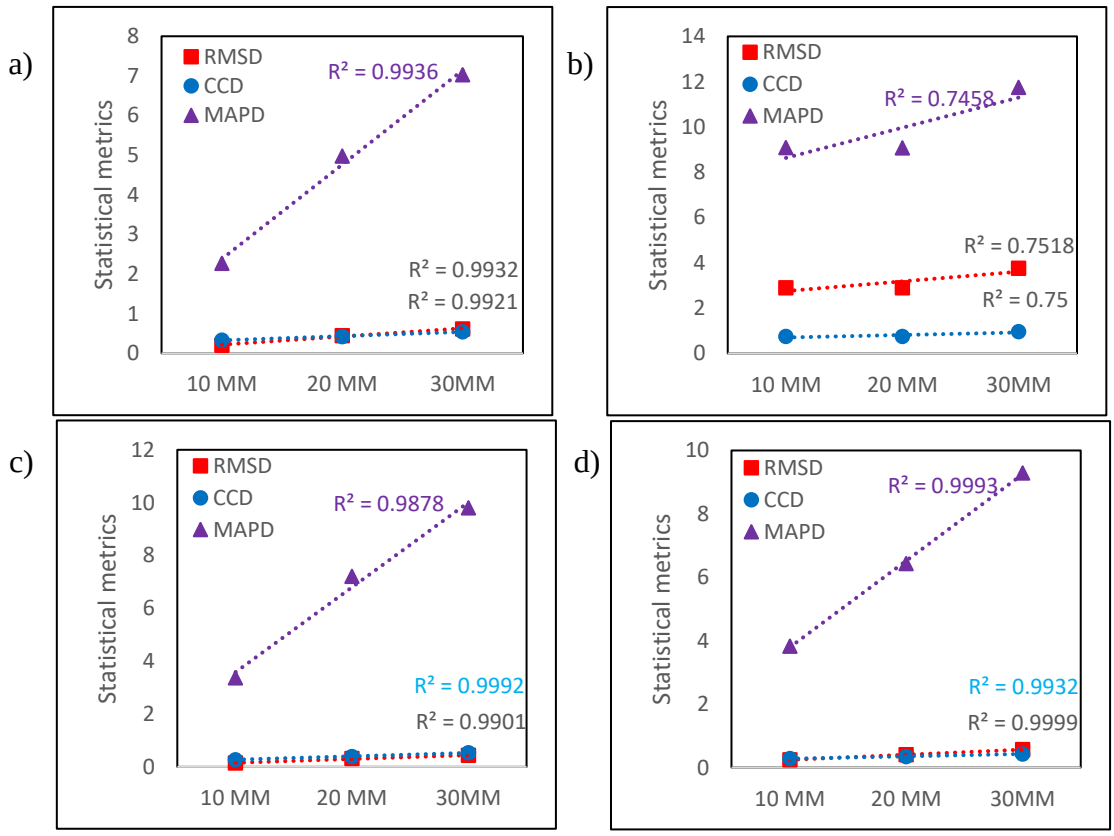

Figure 13. Performance evolution of PZT with SIAU and epoxy (a) first SIAU peak (b) first epoxy peak (c) second SIAU peak (d) second epoxy peak.

IV. CONCLUSIONS

This work presented the analysis of a new set of protection sensors designed to detect damage to mechanical structures based on the SHM approach. Using the data, it was possible to verify:

- The RMSD, MAPD and CCD values increase with notch depth for both epoxy and SIAU, indicating a positive correlation between damage depth and damage detection. However, SIAU proves to be more sensitive to larger and deeper damage ranges, indicating a better response in these scenarios, as assessed by the CCD and MAPD metrics.
- The results of the FEM model are compared in terms of proportion with the experimental analysis for different notch cut levels, showing a similar fit to the simulation, which demonstrates effective validation of the modeling carried out.
- A study with deeper notches is needed to verify the behavior of SIAU in relation to epoxy for damage detection, in order to see if the RMSD values would remain at a lower level or if they would progress as the damage evolved.
- There is a favorable linear correlation of the metrics when only the SIAU set is considered, with better R^2 values at both resonance peaks.

The study demonstrates the efficiency of SIAU in detecting deep damage by analyzing sensitivity at high frequencies. However, to evaluate the behavior and durability of the array, it is recommended to expand the studies to include different environmental conditions. In addition, long-term tests corroborate the understanding of the array behavior. Future research should include tests with deeper notches (> 30 mm), variation in the type of damage, different temperatures and vibration conditions to verify the impact on the metrics.

Another point to be explored is the use of low-cost devices, such as the AD5933, to simplify field application and reduce implementation and data processing costs, the incorporation of additional sensors for environmental compensation and the use of machine learning-based normalization algorithms to reduce false positives caused by variable operating conditions.

ACKNOWLEDGEMENTS

Funding: The authors would like to thank CAPES (Process: 88887.801188/2023) for financially supporting the research work reported in this article through INCT-EIE, and the laboratories LLabEst - Structures Laboratory and LMEst - Structural Mechanics Laboratory.

REFERENCES

[1]. ANAZ, A.; SUBRAMANIAM, K. V. L. Impedance-based damage measurement in concrete using bonded PZT patches. 2014. Dissertação (Mestrado) – Indian Institute of Technology, Hyderabad, 2014.

[2]. CASTRO, BA; BAPTISTA, FG; CIAMPA, F. "Comparative Analysis of Signal Processing Techniques for Impedance-Based SHM Applications in Noisy Environments". mechanical systems and Signal Processing, vol. 126, July 2019, p. 326-40. https://doi.org/10.1016/j.ymssp.2019.02.034

[3]. COMSOL Multiphysics. Reference manual. Available at:<https://doc.comsol.com/5.5/doc/com.comsol.help.comsol /COMSOL_ReferenceManual.pdf>. 10 Dec. 2023.

[4]. ESPINOSA, MCP; Calub, PN; Phenol, DS Simulation of Piezoelectric Stack Actuators for Loss Component. Journal of Engineering Science & Technology Review, [sl], v. 14, no. 4, p. 153-160, 2021.Available at:< http://jestr.org/downloads /Volume14Issue4/fu lltext19144 2021.pdf >. Accessed on: December 10, 2023.

[5]. GAYAKWAD, H.; THIYAGARAJAN, JS Structural Damage Detection through EMI and Wave Propagation Techniques Using Embedded PZT Smart Sensing Units. Sensors, vol. 22, no. 6, p. 2296. https://doi.org/10.3390/s22062296

[6]. LIANG, C.; SUN, F.; ROGERS, CA Coupled electro-mechanical analysis of adaptive material systems - determination of the actuator power consumption and system energy transfer. Journal Intelligent Material Systems and Structures, London, vol. 5, no. 1, p. 12-20, 1994

[7]. LIM, YY Monitoring of concrete hydration using electromechanical impedance technique. Australasian Conference on Mechanics of Structures and Materials (ACMSM 23). 23rd edition, p. 1155-1160, 2014.

[8]. SILVA et al. Impedance-based structural integrity monitoring applied to steel fiber reinforced concrete structures. Revista da Sociedade Brasileira de Ciências Mecânicas e Engenharia, v. 42, n. 7, 30 jun. 2020. https://doi.org/10.1007/s40430-020-02458-4

[9]. SAMANTARAY, S. K. et al. An impedance-based structural health monitoring approach for looseness identification in bolted joint structure. Journal of Civil Structural Health Monitoring, v. 8, n. 5, p. 809-822, 26 sep. 2018. https://doi.org/10.1007/s13349-018-0307-2

[10]. VIEIRA, P. G. Frequency range selection using wavelets for damage detection in SHM systems based on the EMI principle. 114 f. Dissertation (master's) - School of Electrical Engineering, Universidade Estadual Paulista, 2016. https://repositorio.unesp.br/handle/11449/148608

[11]. ZHANG, C.; PANDA, GP; YAN, Q.; ZHANG, W.; VIPULANANDAN C.; SONG, G. Monitoring early-age hydration and setting of Portland cement paste by piezoelectric transducers via electromechanical impedance method. Construction and Building Materials, vol. 258, p. 120348, October 2020. https://doi.org/10.1016/j.conbuildmat.2020.120348.

Authors

Lucas Gomes – Currently pursuing a degree in Computer Engineering at UFU. Graduated in Civil Engineering from UNIPAM and holds a Master's Faculty in Civil Engineering from UFU.

Raquel Naiara Fernandes Silva – Ph.D. in Solid Mechanics and Vibrations from UFU, Master's in Geodetic Sciences from UFPR, and a degree from UFV. Adjunct Professor at UFU's Faculty of Civil Engineering. Researches Structural Health Monitoring (SHM), focusing on Electromechanical Impedance in concrete structures. Experienced in Geodetic Monitoring of Concrete Dams and the application of Geotechnologies in Civil and Environmental Engineering.

Leila Aparecida de Castro Motta – Ph.D. from USP, Master's in Structural Engineering from EESC-USP, and a Civil Engineering degree from UFU. Associate Professor at UFU. Specializes in Construction Materials, focusing on vegetable fibers for reinforced composites and the use of waste in developing new or modified construction materials.